

Cite this: *Chem. Soc. Rev.*, 2012, **41**, 2308–2322

www.rsc.org/csr

CRITICAL REVIEW

## Progress in adsorption-based CO<sub>2</sub> capture by metal–organic frameworks

Jian Liu, Praveen K. Thallapally,\* B. Peter McGrail, Daryl R. Brown and Jun Liu

Received 17th August 2011

DOI: 10.1039/c1cs15221a

Metal–organic frameworks (MOFs) have recently attracted intense research interest because of their permanent porous structures, large surface areas, and potential applications as novel adsorbents. The recent progress in adsorption-based CO<sub>2</sub> capture by MOFs is reviewed and summarized in this *critical review*. CO<sub>2</sub> adsorption in MOFs has been divided into two sections, adsorption at high pressures and selective adsorption at approximate atmospheric pressures. Keys to CO<sub>2</sub> adsorption in MOFs at high pressures and low pressures are summarized to be pore volumes of MOFs, and heats of adsorption, respectively. Many MOFs have high CO<sub>2</sub> selectivities over N<sub>2</sub> and CH<sub>4</sub>. Water effects on CO<sub>2</sub> adsorption in MOFs are presented and compared with benchmark zeolites. In addition, strategies appeared in the literature to enhance CO<sub>2</sub> adsorption capacities and/or selectivities in MOFs have been summarized into three main categories, catenation and interpenetration, chemical bonding enhancement, and electrostatic force involvement. Besides the advantages, two main challenges of using MOFs in CO<sub>2</sub> capture, the cost of synthesis and the stability toward water vapor, have been analyzed and possible solutions and path forward have been proposed to address the two challenges as well (150 references).

Energy and Environment Directorate, Pacific Northwest National Laboratory, Richland, WA 99352, USA.  
E-mail: Praveen.Thallapally@pnnl.gov; Fax: +1-509-371-7249;  
Tel: +1-509-371-7183

### 1 Introduction

The global climate change phenomenon, which is caused mainly by the discharge of CO<sub>2</sub> into the atmosphere, has



Jian Liu

Jian Liu is currently a Postdoctoral Research Associate at the Pacific Northwest National Laboratory (PNNL), USA. His research interests include carbon dioxide capture, metal–organic frameworks (MOFs) synthesis and applications, gas adsorption fundamental and applications, and materials chemistry. Jian received his Bachelor of Engineering degree from Beijing Institute of Technology in 2003 and then in 2006 he obtained a Master of Engineer-

ing degree from Chinese Academy of Sciences. He earned his PhD in Chemical Engineering from the Vanderbilt University in May 2011. Before joining PNNL, Jian was working with Professor M. Douglas LeVan at the Vanderbilt University on adsorption equilibrium and mass transfer in MOF adsorbents. Jian has won the 2011 AIChE Separation Division Graduate Student Research Award in Adsorption and Ion Exchange. Dr Liu has published over 15 peer reviewed papers and presented several talks in four consecutive AIChE Annual Conference. He is also a member of the AIChE and the Sigma Xi Society.



Praveen K. Thallapally

Praveen K. Thallapally obtained his PhD in 2003 from the University of Hyderabad working with Prof. Gautam R. Desiraju on crystal engineering and polymorphism. After graduation he moved to the Prof. Jerry L. Atwood research group at the University of Missouri-Columbia (UMC) as a postdoctoral research associate where he investigated gas storage and separation using porous organic and metal coordination solids. In 2006 he moved

to Pacific Northwest National Laboratory (PNNL) as a Sr. Research Scientist. His research interests include the fundamental understanding of nucleation and crystal growth of nanostructured materials, gas separation, adsorption cooling, separation and immobilisation of radio nuclides (Kr, I<sub>2</sub>), and development of electro-optic responsive MOFs. Dr Thallapally has published over 70 peer reviewed publications and he currently serves as a Community of Board of Editor for Crystal Growth & Design Network and a Topic Editor for Crystal Growth & Design.

attracted more and more attention.<sup>1</sup> Some research results reveal that the concentration of CO<sub>2</sub> in the atmosphere has increased from about 310 ppm to over 380 ppm during the last half century.<sup>2</sup> In the United States, over 94% of the CO<sub>2</sub> emission is from the combustion of carbon-based fossil fuels.<sup>3</sup> The U.S. Department of Energy (DOE) issued a carbon sequestration program in 2009 aiming to achieve 90% CO<sub>2</sub> capture at an increase in the cost of electricity of no more than 35% for the post-combustion process by 2020.<sup>4</sup>

Physisorption between certain adsorbents and CO<sub>2</sub> molecules could allow conveniently reversible processes to capture CO<sub>2</sub> gas. It requires much less energy compared to the conventional techniques that use basic species such as aqueous ammonia and amine functionalized solids to remove CO<sub>2</sub> gas.<sup>5-7</sup>

Activated carbon, carbon molecular sieves, and zeolites have been extensively studied as adsorbents for CO<sub>2</sub> gas.<sup>8-10</sup> The common shortfalls of these traditional adsorbents are either low capacities or difficult regeneration processes.

Metal-organic frameworks (MOFs), also known as coordination networks or coordination polymers, are novel materials constructed by coordinate bonds between multidentate ligands and metal atoms or small metal-containing clusters (referred to as secondary building units or SBU).<sup>11-13</sup> Most of the MOF materials have 3D structures incorporating uniform pores and a network of channels. The integrity of these pores and channels can be retained after careful removal of the guest species. The remaining voids within the 3D structures then can adsorb other guest molecules.<sup>14,15</sup> The structure of a typical MOF, Zn<sub>4</sub>O(O<sub>2</sub>C-C<sub>6</sub>H<sub>4</sub>-CO<sub>2</sub>)<sub>3</sub>, which is known as IRMOF-1 (or MOF-5), is constructed with zinc atoms as metal centers and terephthalic acid molecules as ligands as shown in Fig. 1a. The central cavity formed by the metal centers and ligands is much larger compared to other traditional adsorbents and is essential for gas storage.<sup>14</sup>

Considerable efforts have been expended on the synthesis of MOF materials in the last several years.<sup>16,17</sup> MOFs are synthesized generally by hydrothermal or solvothermal methods. Some novel electrochemical approach has also been reported recently.<sup>18</sup> The state of the art is in the choice of metal centers and design and synthesis of organic ligands. Different combinations of metal centers and organic ligands based on rational design ideas will generate MOF materials with various structures and properties. Besides large surface areas and pore volumes, some MOF materials are well known to have unsaturated metal centers (UMCs),<sup>19-22</sup> such as M-MOF-74 or M/DOBDC (M = Zn, Co, Ni, Mg) shown in Fig. 1b, in their 3D structures which can offer extra and usually strong binding sites to guest molecules.<sup>23,24</sup> In addition, the pore sizes of some MOFs can be adjusted from



**B. Peter McGrail**

*B. Peter McGrail is a staff member at PNNL for over 28 years and has attained the position of Laboratory Fellow, the highest level of scientific achievement at the laboratory. He directs a wide variety of research projects in greenhouse gas emission management, energy efficiency technology development. Dr McGrail manages the Zero Emission Research & Technology Center, which is conducting groundbreaking work on the reactivity of molecular*

*water solvated in supercritical CO<sub>2</sub> among other basic science studies of key importance for designing CO<sub>2</sub> capture and sequestration systems. He has over 220 publications and presentations at international conferences on his research.*



**Daryl R. Brown**

*Daryl Brown obtained his MBA in 1986 and has acquired a broad range of experience directing and performing analyses of advanced technology systems. The majority of this experience has been oriented toward energy generation and storage systems where he has authored or co-authored over 100 publications. Mr Brown specializes in cost estimating and life-cycle costing for all kinds of advanced technologies and has conducted many preliminary*

*engineering feasibility studies incorporating design, performance, cost, and economic analyses.*



**Jun Liu**

*Jun Liu is a Laboratory Fellow at the Pacific Northwest National Laboratory and a leader for the Transformational Materials Science Initiative. He is also a Fellow for the American Association for the Advancement of Science. In the past, he has served as a Pacific Northwest National Laboratory Fellow, senior research staff for Sandia National Laboratories and Lucent Bell Laboratory, Department Manager for the Synthesis and Nanomaterials*

*Department, Sandia National Laboratories, and Thrust Leader for Complex Functional Nanomaterials for the Center for Integrated Nanotechnologies, Sandia National Laboratories. He is recognized for his research in functional nanomaterials and their application for energy and environment. He has received an R & D 100 Award, and he was named 2007 Distinguished Inventor of Battelle. He has over 200 publications and many invited review articles in leading technical journals.*

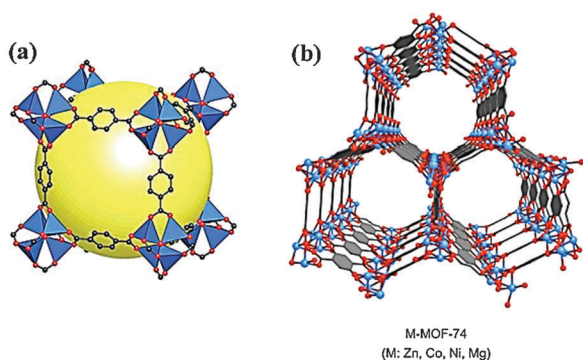


**Fig. 1** The structures of two MOF examples. (a) IRMOF-1. SBU:  $Zn_4O$  tetrahedron, ligands: terephthalic acid, black balls: C atoms, red balls: O atoms, yellow sphere: center cavity. Reproduced from ref. 14. (b) M-MOF-74 or M/DOBDC. M = Zn, Co, Ni or Mg, blue balls: metal atoms, red balls: O atoms, gray stick: C atoms. Reproduced from ref. 22.

several angstroms to a few nanometres by varying the sizes of the organic linkers.<sup>25–27</sup> Moreover, not like inorganic zeolites and porous carbon materials, the properties and functions of the pores can be easily tuned for specific applications by post-synthetic modification of the parent MOFs.<sup>28–31</sup> Besides the large gas capacities at equilibrium states, the adsorption rates in some MOFs are fast which is essential for practical gas separation applications. Generally, self-diffusivities or intracrystalline diffusivities for gas adsorbed in MOFs are larger than in zeolites because of larger pores and open structures in MOF materials.<sup>32–35</sup> Liu *et al.*<sup>36</sup> reported that the main resistance for  $CO_2$  adsorption in HKUST-1 (or CuBTC) and Ni/DOBDC is macropore diffusion. So the  $CO_2$  adsorption rate is generally much faster than  $CO_2$  adsorption in NaX and 5A zeolites where micropore diffusion is the rate control mechanism. Due to the favorable properties mentioned above, MOFs stand out from other porous materials for gas storage and separation applications.

Several reviews have summarized the research efforts in gas adsorption applications for MOFs, such as hydrogen and methane storage, and carbon dioxide capture.<sup>37–42</sup> Recently, Sholl and co-authors<sup>43</sup> contributed a review on experimental applications of MOFs in large-scale carbon dioxide separations in which both adsorption-based and kinetic separations of  $CO_2$  are included. Adsorption-based separations rely on the fact that gases adsorbed in nanopores have much higher densities than those of the gases in bulk phases. Kinetic separations use differences in adsorption affinities and differences in diffusivities of gases in a porous adsorbent. Kinetic separations are often used in membrane-based applications.<sup>44,45</sup> In this review, we will focus on the progress and challenges in using MOFs for adsorption-based  $CO_2$  capture including both experimental and simulation studies. First, research on high pressure  $CO_2$  storage in MOFs will be reviewed. Then, the  $CO_2$  adsorption at sub-atmospheric pressure and selective  $CO_2$  adsorption in MOFs will be presented and analyzed. Next, the key strategies aiming to increase  $CO_2$  capacities and/or selectivities in MOFs will be discussed and summarized into several categories. At last, current challenges toward using MOFs in  $CO_2$  capture, such as cost and stability, will be discussed as well.

## 2 $CO_2$ adsorption in MOFs at high pressures

$CO_2$  storage by adsorbents is an economical and relatively mature method considering the low cost of equipment and the possible recycling uses of the captured  $CO_2$ .<sup>46–48</sup> Millward and Yaghi published a pioneering work in which  $CO_2$  isotherms up to 42 bar were reported for nine MOF materials as shown in Fig. 2.<sup>49</sup>

Several MOFs have higher saturated  $CO_2$  capacities than benchmark adsorbents such as zeolites NaX (or 13X) and activated carbon MAXSORB. Particularly, MOF-177, which is composed of Zn and a large linker 4,4',4''-benzene-1,3,5-triyl-tribenzoic acid ( $H_3BTB$ ), has an unprecedented  $33.5 \text{ mol kg}^{-1}$   $CO_2$  capacity at  $25^\circ\text{C}$  and 35 bar. The authors ascribed this large  $CO_2$  capacity to the large pore space enclosed in MOF-177. Their results also showed that the saturated  $CO_2$  capacities of the MOFs are qualitatively correlated with their surface areas.

MIL-53 (Al) and MIL-53 (Cr) are interesting materials because of their “breathing” crystal structures induced by adsorption of  $H_2O$  molecules as shown in Fig. 3.<sup>50,51</sup> The structure to the left shows the hydrated form in which the pores are slightly deformed due to hydrogen-bond interactions between the hydrogen atoms of the water molecules and the oxygen atoms of the carboxylates and the  $\mu_2$ -hydroxyl groups. After water is removed through heating, the pores will return back to the structure on the right with more open porosity. Bourrelly *et al.*<sup>44–51</sup> found that  $CO_2$  molecules will initially be adsorbed to the hydroxyl groups in MIL-53 (Al) and this will cause shrinkage of the structure. A further increase in the  $CO_2$  pressure will lead to reopening of the pore structure. They reported that MIL-53 (Al) has a  $CO_2$  capacity of  $10.4 \text{ mol kg}^{-1}$

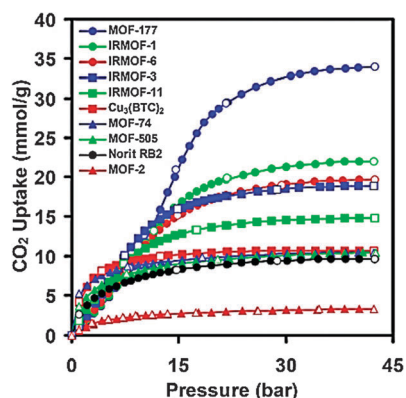


**Fig. 2** Saturated  $CO_2$  capacities for several MOFs determined at ambient temperature. Reproduced from ref. 49.

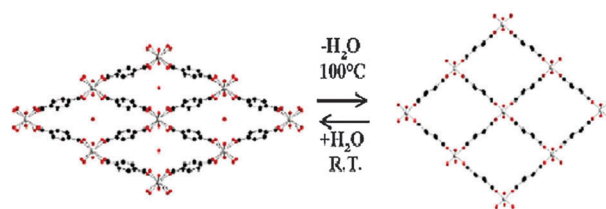


**Fig. 3** Hydration and dehydration processes occurring in MIL-53 (Al, Cr). Left: hydrated structure; right: dehydrated structure. Reproduced from ref. 51.

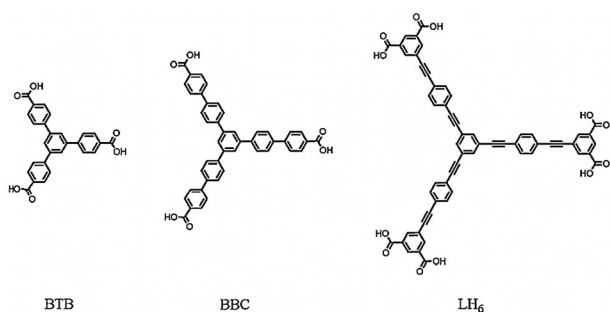


**Fig. 4** Large organic linkers used to synthesize MOFs with extra large surface areas and pore volumes. 4,4',4''-Benzene-1,3,5-triyltribenzoate (BTB) is used to synthesize MOF-177; 4,4',4''-(benzene-1,3,5-triyl-tris (benzene-4,1-diyl))tribenzoate (BBC) is used to synthesize MOF-200; LH<sub>6</sub> is used to synthesize NU-100.

at 30 bar and 304 K, which is well above those of conventional zeolites and comparable with microporous carbons. Substituting Al with Cr in MIL-53 essentially did not cause any change in CO<sub>2</sub> adsorption capacity. Thallapally *et al.*<sup>52</sup> synthesized an interpenetrated MOF which also shows breathing motion upon solvent loss and CO<sub>2</sub> inclusion. This breathing MOF has a CO<sub>2</sub> capacity of 7.1 mol kg<sup>-1</sup> at 30 bar and 298 K, which is similar to that of the NaX zeolites under the same conditions.

Llewellyn *et al.*<sup>53</sup> reported that MIL-101 (Cr), another MOF from Materials of Institute Lavoisier (MIL), shows a high CO<sub>2</sub> capacity, which is about 18 mol kg<sup>-1</sup> at 50 bar and 304 K. Furthermore, the authors activated MIL-101 (Cr) with ethanol and NH<sub>4</sub>F to increase its surface area and pore volume which leads to a record 40 mol kg<sup>-1</sup> CO<sub>2</sub> capacity at 50 bar and 304 K.

Matzger and coauthors<sup>54</sup> synthesized UMCM-1 using zinc nitrate and two different ligands, 1,3,5-tris(4-carboxyphenyl)-benzene (H<sub>3</sub>BTB) and terephthalic acid (H<sub>2</sub>BDC). UMCM-1 has a high surface area (4100 m<sup>2</sup> g<sup>-1</sup>) and giant pore volume (2.141 cc g<sup>-1</sup>). Mu *et al.*<sup>55</sup> measured CO<sub>2</sub> isotherms at three different temperatures for UMCM-1 and they obtained a CO<sub>2</sub> capacity of 23.5 mol kg<sup>-1</sup> at 24 bar and 298 K.

Farha *et al.*<sup>56</sup> used computational modeling to design a metal-organic framework, NU-100, with a particularly high surface area. Then they successfully obtained a matched MOF through the experimental synthesis, with a high BET surface area (6143 m<sup>2</sup> g<sup>-1</sup>). The NU-100 is composed of copper centers and a large hexatopic carboxylate ligand (LH<sub>6</sub>) which is shown in Fig. 4. Furthermore, the NU-100 has a CO<sub>2</sub> capacity of 46.4 mol kg<sup>-1</sup> at 40 bar and 298 K.

Recently, Yaghi and coauthors reported several MOFs with ultra-high porosity.<sup>57</sup> Particularly, MOF-210 exhibits the highest BET and Langmuir surface area (6240 and 10400 m<sup>2</sup> g<sup>-1</sup>) and pore volume (3.60 cc g<sup>-1</sup> and 0.89 cc g<sup>-1</sup>) of MOF materials reported so far. Basically, they achieved the ultra-high porosity by expanding the sizes of organic linkers from terephthalic acid (BDC) in IRMOF-1 to 4,4',4''-(benzene-1,3,5-triyl-tris (benzene-4,1-diyl)) tribenzoate (BBC) in MOF-200. The BBC linker is even larger than 4,4',4''-benzene-1,3,5-triyltribenzoate (BTB) which is used to synthesize MOF-177 as shown in Fig. 4. More importantly, they achieved a new record CO<sub>2</sub> capacity of 54.5 mol kg<sup>-1</sup> at 50 bar and 298 K for MOF-200 and MOF-210. For monodisperse cubic nanoparticles to have an external surface that is equal to these two MOFs, the size of the nanoparticle would have to be only 3 to 6 nm, which may

**Table 1** High-pressure CO<sub>2</sub> adsorption data for selected MOFs

Sample	Surface area/m <sup>2</sup> g <sup>-1</sup>		Pore volume/cc g <sup>-1</sup>	CO <sub>2</sub> uptake/mol kg <sup>-1</sup>	Temperature/K	Pressure/bar	Reference
	BET	Langmuir					
HKUST-1 (CuBTC)	1781	—	—	10.7	298	35	49
IRMOF-1 (MOF-5)	1270	—	0.71	17.5	308	300	58
	2833	—	—	21.7	298	35	49
	—	—	—	10.9	298	14	59
IRMOF-3	2160	—	—	18.7	298	35	49
IRMOF-6	2516	—	—	19.5	298	35	49
IRMOF-11	2096	—	—	14.7	298	35	49
MIL-47 (V)	—	1500	—	11.5	304	20	51
MIL-53 (Al)	—	1500	—	10.4	304	30	51
MIL-53 (Cr)	1300	—	0.42	6.8	298	25	60
	—	1500	—	10.0	304	25	51
MIL-100 (Cr)	1900	—	1.1	18	304	50	53
MIL-101 (Cr) <sup>a</sup>	4230	—	2.2	40	304	50	53
MIL-102 (Cr)	—	—	—	3.1	304	30	61
MOF-2	345	—	—	3.2	298	35	49
MOF-74	816	—	—	10.4	298	35	49
MOF-177	4508	—	—	33.5	298	35	49
	—	—	—	9.0	298	14	59
MOF-200	4530	10400	3.59	54.5	298	50	57
MOF-205	4460	6170	2.16	38.1	298	50	57
MOF-210	6240	10400	3.60	54.5	298	50	57
MOF-505	1547	—	—	10.2	298	35	49
NU-100	6143	—	—	46.4	298	40	56
UMCM-1	4100	—	2.14	23.5	298	24	55
USO-2-Ni	1925	—	0.74	13.6	298	25	60
Zn <sub>4</sub> O(FMA) <sub>3</sub> <sup>b</sup>	1120	1618	—	15.7	300	28	62
Zn <sub>9</sub> O <sub>3</sub> (2,7-ndc) <sub>6</sub> (dmf) <sub>3</sub> <sup>c</sup>	834	1146	0.41	7.1	298	40	63

<sup>a</sup> Activated by ethanol and NH<sub>4</sub>F. <sup>b</sup> FMA: fumarate. <sup>c</sup> 2,7-ndc: 2,7-naphthalene dicarboxylic acid; dmf: dimethylformamide.

not be large enough for practical use. This indicates that the surface areas of MOF-200 and MOF-210 are close to the ultimate limit for solid materials and so is the 54.5 mol kg<sup>-1</sup> CO<sub>2</sub> capacity at 50 bar and 298 K.

Results reported so far about CO<sub>2</sub> adsorption in MOFs at high pressures are summarized in Table 1. It is clear that CO<sub>2</sub> capacities at high pressures depend on surface areas and pore volumes of the MOFs. Increasing surface areas and pore volumes of MOFs is an effective way to enhance their CO<sub>2</sub> storage capabilities. Therefore, many large organic linkers with multiple benzene rings and extended length, such as the BTB and BBC linkers mentioned above, have been used to synthesize MOFs with extra-large surface areas and pore volumes. In addition to tailoring chemical compositions and pore structures such as using larger organic linkers, activating MOFs with supercritical fluid is another option to increase surface areas and pore volumes. Supercritical activation can eliminate the solvent surface tension at temperatures and pressures above the critical point which will prevent the pore collapse that would otherwise occur upon removal of organic solvents by heat. Nelson *et al.*<sup>64</sup> reported that MOFs have much larger surface areas and pore volumes after solvent exchange than after thermal evacuation. Supercritical drying (ScD) can help thoroughly remove residual solvent inside a MOF and increase their surface area to an even larger value than using solvent exchange.

### 3 Sub-atmospheric pressure and selective CO<sub>2</sub> adsorption in MOFs

#### 3.1 CO<sub>2</sub> adsorption at sub-atmospheric pressures

There are at least two applications where separation of CO<sub>2</sub> from other gases using MOFs is of interest. They are separation of CO<sub>2</sub> from sour natural gas wells and separation of CO<sub>2</sub> from power-plant flue gas.<sup>41</sup> The CO<sub>2</sub> partial pressure is much lower than atmospheric pressure for the second application. Therefore, it is important to study CO<sub>2</sub> adsorption in MOFs at sub-atmospheric pressures.

Yazaydin *et al.*<sup>65</sup> used both experiments and simulation to screen MOFs for the highest CO<sub>2</sub> capacities at about 0.1 atm. They found that Mg/DOBDC and Ni/DOBDC (also known as Mg-MOF-74 and Ni-MOF-74 or CPO-27-Mg and CPO-27-Ni) have the highest CO<sub>2</sub> capacities at 0.1 atm and 298 K, which are 5.95 mol kg<sup>-1</sup> and 4.07 mol kg<sup>-1</sup>, among the 14 MOFs that they considered. The results are shown in Fig. 5.

A correlation between the CO<sub>2</sub> capacity and the heat of adsorption at sub-atmospheric pressures for CO<sub>2</sub> adsorption in MOFs was also reported. In contrast to CO<sub>2</sub> adsorption in MOFs at high pressures, there is no correlation between the CO<sub>2</sub> capacity and the surface area or the free volume. Therefore, they concluded that MOFs with a high density of open metal sites, such as Mg/DOBDC and Ni/DOBDC, are promising in CO<sub>2</sub> capture from flue gas in which CO<sub>2</sub> partial pressure is about 0.1 atm. Liu *et al.*<sup>36</sup> found that Ni/DOBDC has a higher CO<sub>2</sub> capacity than NaX and 5A zeolites at 0.1 atm, and 25 °C. In addition, water does not affect CO<sub>2</sub> adsorption in Ni/DOBDC as much as in NaX and 5A zeolites, and it is much easier to remove water from Ni/DOBDC by regeneration. In other words,

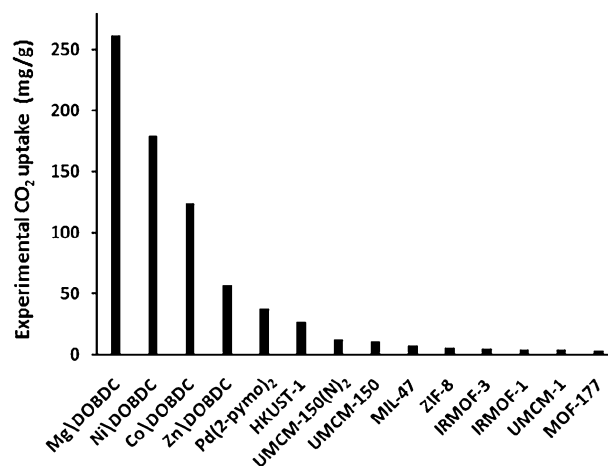


Fig. 5 Experimental CO<sub>2</sub> uptake in different MOFs at 0.1 bar. Data were obtained at 293–298 K. Reproduced from ref. 65.

Ni/DOBDC can adsorb more CO<sub>2</sub> than traditional zeolites under the same moist conditions. Aprea *et al.*<sup>66</sup> reported the CO<sub>2</sub> isotherms at room temperature of CuBTC. Their results showed that CuBTC has a higher CO<sub>2</sub> capacity at atmospheric pressure and a lower isosteric heat of adsorption than zeolites NaX, which means CuBTC could be more suitable for fixed-bed CO<sub>2</sub> adsorption applications than zeolites NaX. Caskey *et al.*<sup>67</sup> found that metal substitution in the DOBDC series can impact their CO<sub>2</sub> capacities at the low-pressure region significantly. This metal substitution effect may be caused by the differences in the ionic character of the metal-oxide bonds in the DOBDC-series MOFs.<sup>65</sup>

#### 3.2 CO<sub>2</sub> adsorption over N<sub>2</sub> and CH<sub>4</sub>

Large capacities at sub-atmospheric pressures are essential for application of MOFs in CO<sub>2</sub> adsorption. However, selectivity is a more important factor since CO<sub>2</sub> is always mixed with other gases in practical applications.<sup>39</sup> The selectivity for gas A relative to gas B is defined by  $S_{AB} = (x_A/x_B)(y_B/y_A)$ , where  $x_A$  and  $x_B$  are the mole fractions of gases A and B in the adsorbed phase, and  $y_A$  and  $y_B$  are the mole fractions of gases A and B in the bulk phase, respectively. Selective adsorption of CO<sub>2</sub> over N<sub>2</sub> has attracted extended attention because of the urgent need to separate CO<sub>2</sub> from flue gas. Similarly, selective adsorption of CO<sub>2</sub> over CH<sub>4</sub> in MOFs is also of interest considering the potential application in natural gas upgrade. Although we will try to address CO<sub>2</sub>/N<sub>2</sub> and CO<sub>2</sub>/CH<sub>4</sub> adsorption in MOFs in sequence, it is not necessary nor our purpose to treat them as two distinct topics because many research studies have investigated both the CO<sub>2</sub>/N<sub>2</sub> and CO<sub>2</sub>/CH<sub>4</sub> separations together.

Li *et al.*<sup>68</sup> synthesized a robust zeolitic MOF material that selectively adsorbs CO<sub>2</sub> over N<sub>2</sub>. This selectivity may be due to the small channels in the zeolitic MOF, which distinguish the two gases with kinetic diameters (CO<sub>2</sub>, 3.3 Å; N<sub>2</sub>, 3.64 Å) similar to the molecular sieve effect observed in zeolites 4A. Seven MOFs, including CuBTC, MIL-47 (V), IRMOF-1, IRMOF-12, IRMOF-14, IRMOF-11, and IRMOF-13, were studied for the separation performance of CO<sub>2</sub> over N<sub>2</sub> by Liu and Smit using Grand Canonical Monte Carlo (GCMC) simulations.<sup>69</sup> In all the

MOFs they considered, CO<sub>2</sub> is more preferentially adsorbed than N<sub>2</sub> with CuBTC showing the highest selectivity. IRMOF-1, IRMOF-12, and IRMOF-14 with large cubic pores give the lowest CO<sub>2</sub>/N<sub>2</sub> adsorption selectivities up to 20 bar. They found that pore size plays an important role in the selective adsorption of CO<sub>2</sub> over N<sub>2</sub> and the reason is that both CO<sub>2</sub> and N<sub>2</sub> molecules have quadrupole moments so the electrostatic interactions will help increase the adsorption of both components. The effect of the chemistry of the materials, *i.e.* effects of the electrostatic interaction, becomes less evident compared to the effects of pore size on selective adsorption of CO<sub>2</sub> over N<sub>2</sub>. Wu *et al.*<sup>70</sup> constructed a Li-modified IRMOF-1, chem-4Li MOF, which was obtained by substituting all the hydrogen atoms by O–Li groups in the aromatic rings of IRMOF-1 as shown in Fig. 6. The chem-4Li MOF was found to have a CO<sub>2</sub>/N<sub>2</sub> selectivity of 395 (CO<sub>2</sub> : N<sub>2</sub> = 15.6 : 84.4), which is two orders of magnitude larger than that of the original IRMOF-1. The main reason is due to the stronger electrostatic interactions between the framework atoms and the gas molecules induced by the introduction of lithium. Yang *et al.*<sup>71</sup> reported a similar enhanced CO<sub>2</sub> selectivity phenomenon for Li modified IRMOF-16.

MIL-53 (Al) is known as a MOF that has flexible structures, which can affect CO<sub>2</sub> adsorption. As mentioned before, besides hydration, adsorption of CO<sub>2</sub> leads to contraction of the MIL-53 (Al) framework and formation of a narrow pore. Finsy *et al.*<sup>72</sup> found that up to 5 bar, CO<sub>2</sub> strongly interacts with the framework hydroxyl groups in MIL-53 (Al), while CH<sub>4</sub> is adsorbed in an unselective way. Further adsorption of CO<sub>2</sub> molecules at higher pressures reopens the framework and the adsorption mechanism become unselective. As a result, the average separation factor between CO<sub>2</sub> and CH<sub>4</sub> decreases from 7 to 4. In order to improve the selectivity of CO<sub>2</sub>/CH<sub>4</sub> in MIL-53(Al), Couck *et al.*<sup>73</sup> synthesized amino-MIL-53 (Al) using 2-aminoterephthalic acid as the linker and the presence of the amino groups together with the hydroxyl groups drastically enhances the affinity for CO<sub>2</sub>, resulting in an almost infinite selectivity of CO<sub>2</sub>/CH<sub>4</sub> according to their experimental data.

HKUST-1 is another MOF that has been extensively studied for CO<sub>2</sub> adsorption. Yang and Zhong<sup>74</sup> found that the HKUST-1 has ordered microdomains with different electrostatic field strengths in its structure, which can greatly enhance the separation of CO<sub>2</sub>/CH<sub>4</sub> because the two components have largely different electrostatic interactions with the HKUST-1. Martin-Calvo *et al.*<sup>75</sup> simulated the CO<sub>2</sub>/CH<sub>4</sub> adsorption process in HKUST-1 and they reported that the siting of

the molecules in HKUST-1 provided the high adsorption selectivity towards CO<sub>2</sub>. However, Hamon *et al.*<sup>76</sup> did not observe a significant influence of the adsorption sites on the CO<sub>2</sub> selectivity at low pressure in their experimental results. Hamon and coauthors also measured a CO<sub>2</sub> delta loading of 7.37 mol kg<sup>-1</sup> between the production step at 1.0 MPa and the regeneration step at 0.1 MPa for the CO<sub>2</sub>–CH<sub>4</sub>–CO (70–15–15) separation by using HKUST-1. This selectivity is significantly higher than that of zeolite NaX and activated carbon under the same conditions.

Keskin and Sholl<sup>77</sup> predicted that IRMOF-1 has a CO<sub>2</sub>/CH<sub>4</sub> selectivity of 2.5 based on their simulation results of a mixture composed of equal parts of CO<sub>2</sub> and CH<sub>4</sub>. They also found that mixture effects significantly affect the CO<sub>2</sub>/CH<sub>4</sub> selectivity for IRMOF-1 under conditions relevant for natural-gas applications. Therefore, examining only single component gases will not be sufficient for understanding the properties of MOFs in practical CO<sub>2</sub> separation applications. Perez *et al.*<sup>78</sup> found that mixing 30% IRMOF-1 with a Matrimid<sup>®</sup> polymer can enhance the CO<sub>2</sub>/CH<sub>4</sub> selectivity of IRMOF-1 to 29 at 308 K and 2 bar. Other than mixing with a polymer, the selectivity of CO<sub>2</sub> from CO<sub>2</sub>/CH<sub>4</sub> mixtures is greatly increased for IRMOF-1 by introducing lithium ions into its structure. This enhancement is due to the electrostatic potential in the materials caused by the presence of the metals.<sup>79</sup> Recently, experimental evidence has been reported by Bae *et al.*<sup>80</sup> to show that Li doping can help improve the CO<sub>2</sub>/CH<sub>4</sub> selectivity to about 50 for some Zn-based mixed-ligand MOFs. They proposed two ways to incorporate Li cations into MOFs, chemical reduction or cation exchange. For the chemical reduction case, the increases in selectivity can be explained by the favorable displacement of catenated frameworks, as well as pore-volume diminution. Conversely, the selectivity enhancement is due to the desolvated-Li(charge)/CO<sub>2</sub>(quadrupole) interactions for the cation exchange method.

Another interesting MOF, Mg/DOBDC, has been recently studied for CO<sub>2</sub> and CH<sub>4</sub> adsorption.<sup>81</sup> The authors found that its CO<sub>2</sub> adsorption capacity is significantly higher than that of zeolite 13X under similar conditions but the pressure-dependent equilibrium selectivity of CO<sub>2</sub> over CH<sub>4</sub> in Mg/DOBDC showed a trend similar to that of zeolite 13X. The authors used the Langmuir model to fit both pure CO<sub>2</sub> and pure CH<sub>4</sub> isotherms. The intrinsic selectivity of CO<sub>2</sub> over CH<sub>4</sub> for Mg/DOBDC at zero adsorption loading is calculated to be 283 at 298 K based on the isotherm data and the Langmuir model parameters.

Selected results about the selectivities of CO<sub>2</sub>/N<sub>2</sub> and CO<sub>2</sub>/CH<sub>4</sub> for some MOFs are shown in Table 2. Some results of the zeolitic imidazolate frameworks (ZIFs), a subclass of MOFs, were also included for reference. It is obvious that many MOFs have high CO<sub>2</sub>/N<sub>2</sub> and CO<sub>2</sub>/CH<sub>4</sub> selectivities which are essential for CO<sub>2</sub> separation from natural gas and flue gas. However, as pointed out by Sholl and coauthors, it is not intrinsically interesting that MOFs preferentially adsorb CO<sub>2</sub> over CH<sub>4</sub> or N<sub>2</sub> because all the microporous adsorbents such as zeolites and activated carbon do unless that a MOF's adsorption selectivity and/or capacity do substantially improve upon traditional and inexpensive adsorbents.<sup>43</sup>

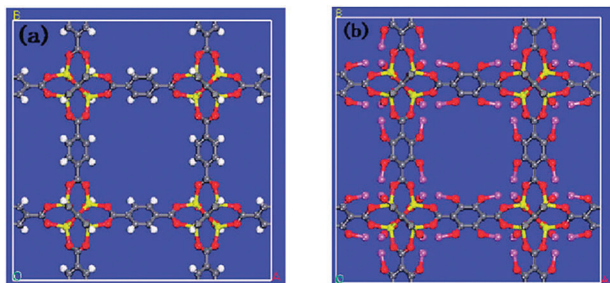


Fig. 6 Structures of IRMOF-1 (a) and chem-4Li MOF (b) (Zn, yellow; O, red; C, gray; H, white; Li, purple). Reproduced from ref. 70.

**Table 2** Selective CO<sub>2</sub> adsorption in some MOFs

Sample	Selectivity			Experiment or Simulation (E or S)	Temperature/K	Pressure/bar	Reference
	CO <sub>2</sub> /CH <sub>4</sub>	CO <sub>2</sub> /N <sub>2</sub>	CO <sub>2</sub> concentration (%)				
Bio-MOF-11	—	36	15	S	298	1	82
Cu(BDC-OH)	6.7 <sup>a</sup>	—	—	S	296	—	83
Cu <sub>2</sub> (Hbtb) <sub>2</sub>	12.4	—	50	E	298	1	84
HKUST-1 (CuBTC)	5	—	50	E	303	1	85
	4	—	50	S	298	1	75
	—	32	50	S	298	10	86
	6	—	50	E	303	1	76
	—	21	50	S	298	2.5	69
	8.5	—	50	S	298	10	74
IRMOF-1 (MOF-5)	2	—	50	S	298	1	75
	29 <sup>b</sup>	—	50	E	308	2	78
	—	3	50	S	298	2.5	69
	2	—	50	S	298	10	74
	2.5 <sup>c</sup>	—	50	S	298	10	77
	—	11	50	S	298	2.5	69
IRMOF-11	—	11	50	S	298	2.5	69
IRMOF-12	—	3	50	S	298	2.5	69
IRMOF-13	—	11	50	S	298	2.5	69
IRMOF-14	—	3	50	S	298	2.5	69
IRMOF-1-4Li (chem-4Li MOF)	—	395	15.6	S	298	1	70
IRMOF-16-4Li	75	—	10	S	298	10	79
Li-MOF	—	60	15	S	298	1	87
Mg/DOBDC (Mg-MOF-74)	283 <sup>d</sup>	—	—	E	298	1	81
MIL-47 (V)	—	10	50	S	298	2.5	69
MOF-508b	3	4	50	S	303	1	88
rho-ZMOF	80	—	50	S	298	1	89
	—	500	15	S	298	1	89
ZIF-68	5	18.7	50	E	298	1	90
ZIF-69	5.1	19.9	50	E	298	1	90
ZIF-70	5.2	17.3	50	E	298	1	90
ZIF-78	10.6	50.1	50	E	298	1	90
ZIF-79	5.4	23.2	50	E	298	1	90
ZIF-81	5.7	23.8	50	E	298	1	90
ZIF-82	9.6	35.3	50	E	298	1	90
ZIF-95	4.3	18	50	E	298	1	90
ZIF-100	17.3	5.9	50	E	298	1	90
Zn (BDC) (TED) <sub>0.5</sub> <sup>e</sup>	4.5	—	50	S	298	1	91
Zn <sub>2</sub> (bpdc) <sub>2</sub> (bpee)(DMF) <sub>2</sub> <sup>f</sup>	257	—	—	E	298	0.16	92
—	—	116	—	E	298	1	90
Zn <sub>2</sub> (NDC) <sub>2</sub> (DPNI) <sup>g</sup>	8 <sup>h</sup>	—	—	S	296	5	93
Zn <sub>3</sub> (OH)(L) <sub>2.5</sub> (DMF) <sub>4</sub> <sup>i</sup>	3.2	14.3	50	E	273	1.05	94
Zn <sub>4</sub> (OH) <sub>2</sub> (1,2,4-btc) <sub>2</sub>	4.5 <sup>a</sup>	—	50	E	295	1	84

<sup>a</sup> Henry's law selectivity. <sup>b</sup> 30% IRMOF-1 in Matrimid<sup>®</sup> polymer. <sup>c</sup> combined with kinetic selectivity. <sup>d</sup> intrinsic selectivity. <sup>e</sup> BDC: benzenedicarboxylate; TED: triethylenediamine. <sup>f</sup> bpdc: 4,4-biphenyl dicarboxylate; bpee: 1,2-bis(4-pyridyl)ethylenelene; DMF: dimethylformamide. <sup>g</sup> NDC: 2,6-naphthalenedicarboxylate; DPNI: *N,N*-di-(4-pyridyl)-1,4,5,8-naphthalene tetracarboxydiimide. <sup>h</sup> Ideal adsorbed solution theory (IAST) predicted selectivity. <sup>i</sup> L: 2,5-dichloro-1,4-benzenedicarboxylate; DMF: dimethylformamide.

### 3.3 H<sub>2</sub>O effects on CO<sub>2</sub> adsorption

Selectivity between H<sub>2</sub>O and CO<sub>2</sub> is important for using MOFs to separate CO<sub>2</sub> from flue gas. However, little research has been done on CO<sub>2</sub>/H<sub>2</sub>O mixture adsorption. Liu *et al.*<sup>36</sup> reported CO<sub>2</sub> isotherms for HKUST-1 and Ni/DOBDC with different amounts of preloaded water. Although they found that water does not affect CO<sub>2</sub> adsorption in HKUST-1 and Ni/DOBDC as much as in traditional zeolites, those two MOFs strongly adsorb water as indicated by their steep water isotherms. Moreover, neither HKUST-1 nor Ni/DOBDC can adsorb any significant amount of CO<sub>2</sub> when water loadings are high which means that the two MOFs preferentially adsorb H<sub>2</sub>O over CO<sub>2</sub>. This is due to the strong interactions between water molecules and the UMCs in HKUST-1 and Ni/DOBDC.

Some interesting results reported in the literature show that a small amount of water can help enhance CO<sub>2</sub> adsorption in

HKUST-1.<sup>95</sup> The enhanced CO<sub>2</sub> uptake is caused by interactions between the quadruple moment of CO<sub>2</sub> and the electric field created by the coordinated water molecules. However, further increasing water loading on the HKUST-1 will result in considerable uncoordinated water molecules that block pore space and make the HKUST-1 adsorb less CO<sub>2</sub> than the dry sample. Chen *et al.*<sup>96</sup> studied the water effects on CO<sub>2</sub> and CH<sub>4</sub> adsorption in MIL-101 (Cr) using molecular simulation. They found that the terminal water molecules in the hydrated MIL-101 provide additional interaction sites and enhance gas adsorption at low pressures. This enhancement is more pronounced for CO<sub>2</sub> than for CH<sub>4</sub>, because the CO<sub>2</sub> molecule has a strong quadruple. However, terminal water molecules reduce free volume and gas adsorption at high pressures.

Liu *et al.*<sup>97</sup> reported that the DOBDC series of MOFs are prone to lose their CO<sub>2</sub> capacities after water adsorption.

In addition, Kizzie *et al.* observed significant decreases in CO<sub>2</sub> capacities for the Mg/DOBDC and Zn/DOBDC which were regenerated after full hydration.<sup>98</sup> The water stability of MOFs will be discussed more in this paper.

## 4 Strategies to enhance CO<sub>2</sub> adsorption in MOFs

The most important criterion to select an adsorbent is having a desired gas capacity at certain pressures.<sup>99</sup> Obviously, high CO<sub>2</sub> capacity and high CO<sub>2</sub> selectivity are desired for the applications of MOFs in CO<sub>2</sub> capture. Extensive research works have been done to make CO<sub>2</sub> adsorption favorable in MOFs and can be summarized into three main categories: catenation and interpenetration, chemical bonding enhancement, and electrostatic force involvement.

### 4.1 Catenation and interpenetration

The size of a pore is found to be critical to the adsorption affinity for light gases.<sup>100–102</sup> Within a certain range, a slight variation in pore size can cause a dramatic change in the adsorption affinity for an adsorbate. It has been reported that at low pressures, CO<sub>2</sub> uptake in a MOF correlates with the heat of adsorption, an index of adsorption affinity which depends on the size of a pore.<sup>33,103</sup>

The interpenetration or catenation of two or more frameworks has traditionally been considered as an obstacle to producing highly porous frameworks due to the resultant reduction of pore volume. However, the catenation of two or more frameworks with minimal displacement was found to possibly prevent some MOFs from collapse.<sup>104</sup> Recently, it has been reported that interpenetration and catenation is an effective way to reduce the pore dimensions of IRMOFs as shown in Fig. 7.<sup>105</sup> The catenated IRMOFs such as IRMOF-9, IRMOF-11, and IRMOF-13 have larger CO<sub>2</sub> over CH<sub>4</sub> selectivity compared with their noninterpenetrated counterparts.<sup>106</sup> Keskin and Sholl<sup>107</sup> also found similar results. The enhanced CO<sub>2</sub> selectivity is considered as a result of additional

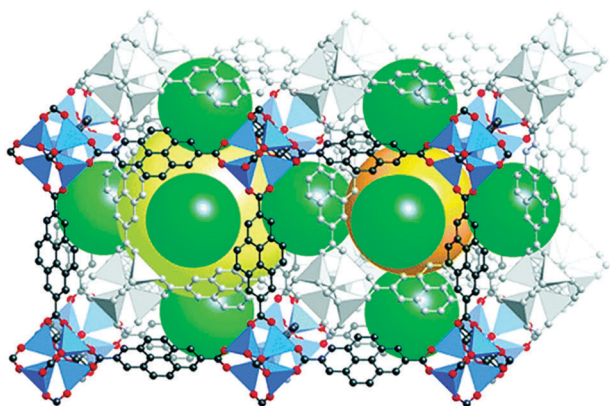


**Fig. 7** Schematic representation of the pore structure in IRMOF-13. The catenation of two frameworks, one shown in grayscale, reduces the fixed diameters of the large and small pores defined by either framework alone. Additional smaller voids are formed, shown as green spheres, which account for roughly 45% of the pore volume. Atom colors: C, black; O, red; Zn, blue tetrahedra; H, not shown. Reproduced from ref. 105.

small pores and adsorption sites formed by the interpenetration of framework. Cheon *et al.*<sup>108</sup> prepared a doubly interpenetrated Mg-based porous MOF with 3D channels. The desolvated solid SNU-25 exhibits high thermal stability and can selectively adsorb CO<sub>2</sub> over CH<sub>4</sub> at various temperatures.

Recently, Kim *et al.*<sup>109</sup> reported that they can synthesize either a catenated (CuTATB-60) or a non-catenated (CuTATB-30) MOF through a sonochemical route by adjusting the ultrasonic power levels. Catenation in CuTATB-60 led to both higher surface area and enhanced stability of the network than the non-catenated counterpart, CuTATB-30. Moreover, the CuTATB-60 showed higher CO<sub>2</sub> adsorption capacity (189 mg g<sup>-1</sup>) than the CuTATB-30 and has an excellent selectivity over N<sub>2</sub> (larger than 20 : 1) as well. Zhang *et al.*<sup>110</sup> synthesized a pillared MOF in both interpenetrated and noninterpenetrated forms and they found that high temperature and reagent concentration favored an interpenetrated crystal form.

### 4.2 Chemical bonding enhancement

One of the chemical bondings that can enhance CO<sub>2</sub> adsorption is a hydrogen-bond interaction between a CO<sub>2</sub> molecule and a MOF structure. Ramsahye *et al.*<sup>111,112</sup> found that in both narrow and large pore versions of MIL-53 (Al) and MIL-53 (Cr), the adsorption mechanism is mainly governed by the interactions between CO<sub>2</sub> molecules and the  $\mu_2$ -OH groups as shown in Fig. 8. The heats of adsorption are over 40 kJ mol<sup>-1</sup> for both MIL-53 (Al) and MIL-53 (Cr). The importance of the  $\mu_2$ -OH group in forming the hydrogen-bond interactions with CO<sub>2</sub> molecules is clearly emphasized by a direct comparison of the behavior of the  $\mu_2$ -OH-containing MIL-53 and the MIL-47 material in which this feature is absent. Serre *et al.*<sup>113</sup> showed that the large breathing effect observed in the MIL-53 structure is due to the existence of OH groups. Vimont *et al.*<sup>114</sup> observed spectroscopic evidence for the formation of electron donor–acceptor complex between CO<sub>2</sub> molecules and hydroxyl groups in the nanoporous hybrid solid MIL-53(Cr) material. Mu *et al.*<sup>115</sup> showed that the incorporation of the electron-donating groups into the organic linkers can largely enhance the adsorption selectivity of MOFs for CO<sub>2</sub>/CH<sub>4</sub> mixture separation through GCMC simulations. This enhancement becomes more evident with the increase of the electron-donating ability of the decorated group while almost no influence by decorating with electron-withdrawing groups. This result helps verify that the CO<sub>2</sub> molecule plays as an electron-acceptor in the electron donor–acceptor complex process.<sup>114</sup>

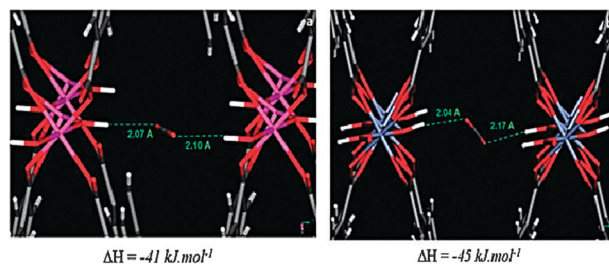


**Fig. 8** Interaction of one CO<sub>2</sub> molecule with two  $\mu_2$ -OH groups on opposing sides of the pore wall in the MIL-53 narrow pore structure containing Al (a) and Cr (b). Reproduced from ref. 112.

Another well-studied method to introduce chemical bonding with CO<sub>2</sub> molecules into MOFs is functionalization by amine and its derivatives. This functionalization can be applied during and after synthesis processes.

Basically, organic linkers containing amine groups are used to functionalize MOFs during the synthesis. Vaidhyanathan *et al.*<sup>116</sup> synthesized an amine-functionalized MOF with zinc carbonate, 3-amino-1,2,4-triazole and oxalic acid. The 3-D framework is built from the pillaring of Zn-aminotriazolate layers by the oxalate groups while the amino groups remain free. In addition, this amine-functionalized MOF preferentially adsorbs CO<sub>2</sub> at low pressures with a 40.8 kJ mol<sup>-1</sup> heat of adsorption. Demessence *et al.*<sup>117</sup> obtained an alkylamine functionalized MOF with 1,3,5-tris(1*H*-1,2,3-triazol-5-yl)benzene (H<sub>3</sub>BTTri) as shown in Fig. 9. The functionalized framework exhibits a higher uptake of CO<sub>2</sub> at very low pressures compared with the nongrafted material and displays a record isosteric heat of adsorption of 90 kJ mol<sup>-1</sup>. Zheng *et al.*<sup>118</sup> successfully constructed a new highly porous rht-type MOF by using a flexible hexacarboxylate ligand with amide linking groups. Their MOF exhibits high surface area, large CO<sub>2</sub> gas storage capacity, and a high heat of adsorption. These observations indicate that decoration of a MOF with polar acrylamide groups can significantly enhance CO<sub>2</sub> binding ability and selectivity of MOFs.

Post-synthetic amine functionalization is also reported in the literature. Wang *et al.*<sup>119</sup> treated DMOF-1-NH<sub>2</sub>, a MOF constructed from Zn(II)-based paddle-wheel secondary building units, 1,4-benzenedicarboxylate, and pillaring 1,4-diazabicyclo[2.2.2]octane (Dabco) ligands, with linear alkyl anhydrides and converted the amine group to the corresponding amide groups. The amide containing MOF has different breathing behavior from the amine containing MOF and also has good CO<sub>2</sub> capacity. An *et al.*<sup>120</sup> synthesized an adenine-containing MOF, bio-MOF-11, which has a high CO<sub>2</sub> capacity and impressive selectivity for CO<sub>2</sub> over N<sub>2</sub>. The authors attribute these favorable CO<sub>2</sub> adsorption properties to the presence of the Lewis basic amino and pyrimidine groups of

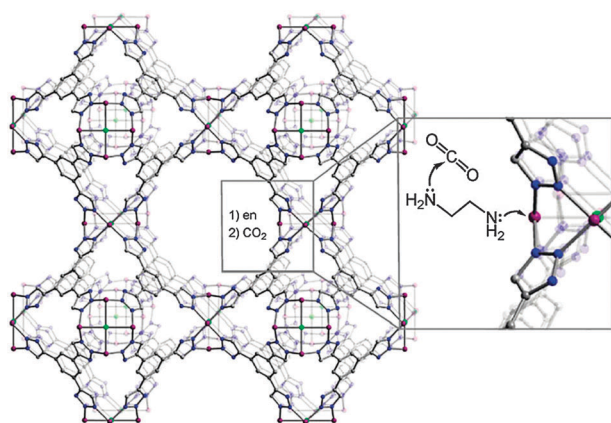


**Fig. 9** A portion of the structure of the sodalite-type framework of Cu-BTTri showing surface functionalization of a coordinatively unsaturated Cu site with ethylenediamine, followed by attack of an amino group on CO<sub>2</sub>. Purple, green, gray, and blue spheres represent Cu, Cl, C, and N atoms, respectively; framework H atoms are omitted for clarity. Reproduced from ref. 117.

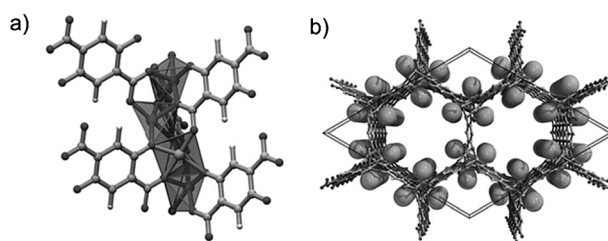


**Fig. 10** (a) Cutout along the chains of the DOBDC series of MOFs showing the coordinatively unsaturated metal atoms in the form of the square-pyramidally coordinated metal centers; (b) crystal structure of the DOBDC series of MOFs viewed along the channels illustrating the primary adsorption sites at the unsaturated metal centers as large spheres. Reproduced from ref. 123.

adenine and the narrow pore dimensions of bio-MOF-11. In addition, the authors introduced tetramethylammonium (TMA), tetraethylammonium (TEA), and tetrabutylammonium (TBA) *via* cation exchange into the pores of bio-MOF-11.<sup>121</sup> They showed that such modifications can be used to systematically tune the CO<sub>2</sub> adsorption capacity of this material and they also suggested that smaller pores in MOFs may be ideal for condensing CO<sub>2</sub> at temperatures relevant to real-world application.

UMCs basically provide coordination bonding sites for CO<sub>2</sub> molecules. Bae *et al.*<sup>122</sup> studied the separation of CO<sub>2</sub>/CH<sub>4</sub> mixtures in a carborane based MOF with and without UMCs. A high selectivity of about 17 between CO<sub>2</sub> and CH<sub>4</sub> was achieved for the MOF with UMCs. This result strongly suggests that UMCs can aid in the separation of (quadru)polar/nonpolar pairs such as CO<sub>2</sub>/CH<sub>4</sub>. Dietzel *et al.*<sup>123</sup> reported that DOBDC series of MOFs contain a large amount of open metal sites, which impart a high affinity towards adsorption of guest molecules as shown in Fig. 10. They observed large CO<sub>2</sub> capacities, quantitative separation of CO<sub>2</sub> from N<sub>2</sub>, and substantial retention of CO<sub>2</sub> in mixtures with CH<sub>4</sub> for Ni/DOBDC and Mg/DOBDC. As a consequence, these MOFs may be eminently suitable for application in separation processes. Recently, Sumida *et al.*<sup>124</sup> synthesized an iron-based MOF, Fe-BTT. They identified that the strongest binding sites reside very close to the framework Fe<sup>2+</sup> cation. The exposed Fe<sup>2+</sup> cation sites within Fe-BTT also lead to the selective adsorption of CO<sub>2</sub> over N<sub>2</sub>. Besides metal atoms, some nonmetal atoms can also form unsaturated centers. Lin *et al.*<sup>125</sup> found that even partially exposed uncoordinated nitrogens can effectively enhance the CO<sub>2</sub> binding affinity in their metal azolate frameworks (MAFs).

### 4.3 Electrostatic force involvement

Electrostatic force is generally introduced into MOF structures through metal ions doping and polar species modification. Babarao *et al.*<sup>126</sup> used molecular simulations to study the adsorption and separation of CO<sub>2</sub>/CH<sub>4</sub> mixture. They found that the presence of extra framework ions can enhance the interactions with guest molecules and act as additional adsorption sites. The adsorption selectivity of CO<sub>2</sub> over CH<sub>4</sub> in charged soc-MOFs is predicted to be one order of magnitude greater than in IRMOF structure and the highest among the various MOFs reported to date. Botas *et al.*<sup>127</sup> doped the IRMOF-1 with Co metal ions and they found that the Co doped materials have

higher adsorption capacities for CO<sub>2</sub> and CH<sub>4</sub> at high pressure than their Co-free homologue. They ascribed the high CO<sub>2</sub> capacity to the exposed Co sites. Their study opens the possibility of doping different MOFs with a variety of metal ions during solvothermal crystallization. Xiang *et al.*<sup>128</sup> showed that the CO<sub>2</sub> and CH<sub>4</sub> adsorption capacities are improved by doping the carbon nanotube modified HKUST-1 with Li. To achieve the enhancement, the Li content must be maintained at an appropriately low concentration because excessive Li doping leads to deformation of the frameworks. Bae *et al.*<sup>129</sup> used a post-synthetic method to modify a Zn-paddlewheel MOF by replacing coordinated solvent molecules with highly polar ligands, 4-(trifluoromethyl) pyridine. This modification introduces electrostatic force into the MOF structure and leads to considerable enhancement of the CO<sub>2</sub>/N<sub>2</sub> selectivity.

## 5 Challenges and outlook

Many MOFs have higher CO<sub>2</sub> capacities than traditional zeolites and some MOFs can selectively adsorb CO<sub>2</sub> from mixtures with N<sub>2</sub> or CH<sub>4</sub> at both sub-atmospheric pressures and high pressures. More importantly, it is much easier to tailor the pore structures and the chemical compositions of MOFs than zeolites. This critical advantage endows considerable possibilities for researchers to increase CO<sub>2</sub> capacity and selectivity for MOFs in the future. However, there are still some existing challenges, such as synthesis cost and material stability, which have to be addressed in order to use MOFs in practical applications.

### 5.1 Synthesis cost of MOFs

Synthesis cost is always a critical issue to consider for practical applications of synthetic materials. Similar to the synthetic zeolites, MOFs are usually synthesized through hydrothermal or solvothermal reactions. The total cost to synthesize a MOF includes the cost of reactors, the cost of reagents, the cost of utilities, and the cost of separation and activation of final products. The reagents usually include metal source, organic linkers, solvents for reactions, and solvents for exchange processes. Compared to the synthetic zeolites, the cost of reactors and the cost of utilities to synthesize MOFs can be assumed to be comparable. Moreover, to prepare MOFs does not need additional capital investment into a totally new technology. Simply adaptation of conventionally available precipitation and crystallization manufacturing methods is feasible.<sup>18</sup> However, the cost of organic linkers and solvents to synthesize MOFs differentiate them from the synthetic zeolites. The organic linkers are usually aromatic compounds which have several benzene rings in their structures with functional groups such as carboxylic acid group, hydroxyl group, and amine group. In addition, imidazole and its derivatives are also used as organic linkers to synthesize a series of MOFs which have zeolitic structures, namely zeolite imidazolate frameworks (ZIFs). Many of the organic linkers have not been commercialized in large scale yet and can only be synthesized in the research labs. To synthesize those special molecules is very costly and time consuming. The cost of organic linkers can be reduced if some new synthesis technology can be developed and adopted in the future to make use

of petroleum raw materials that contain abundant aromatic compounds and minimize the usage of fine chemical reagent.

In order to remove residual solvents remaining inside of the pores and increase the surface areas and pore volumes of MOFs, solvent exchange procedures are usually used to activate the as-synthesized MOFs. Large amounts of organic solvents are consumed in this step and the recovery processes of the solvents are energy intensive. An alternative way to activate MOFs after synthesis is using a supercritical drying technique. According to the literature, using the supercritical drying method can increase the surface areas of MOFs to an even larger value than using solvent exchange followed by thermal regeneration.<sup>64</sup> Taking advantage of using the supercritical drying technique can significantly reduce the use of solvent to activate MOFs thus may reduce the total cost to synthesize MOF materials.

To reduce the cost to synthesize per unit of MOFs, scaling up the synthesis process is a natural choice. Moreover, being able to synthesize MOFs in bulk is a necessity for their applications in CO<sub>2</sub> capture from flue gas considering the scale of the problem. The cost of the raw materials required to synthesize MOFs was determined as a first step toward calculating the MOFs production cost. Costs of the starting materials to produce some MOFs are shown and compared with some normal adsorbents in Table 3. Price quotes were obtained from multiple vendors for each raw material based on the purchase of one metric ton or greater quantity. Prices for individual materials were combined based on the relative amounts required for the synthesis of each MOF to arrive at the raw material cost per MOF. Examining the raw material costs is an easy first step toward estimating MOF production cost and identifies the absolute minimum possible cost for a MOF. This information can be used as an early screening criterion for applications where material costs are expected to be a significant fraction of the total system cost. BASF has recently commercialized four MOF materials, including BASOLITE-A100 (MIL-53), BASOLITE-C300 (HKUST-1), BASOLITE-Z1200 (ZIF-8), and BASOLITE-F300.<sup>18</sup> The retail prices for those commercialized MOFs are from 10 to 15 US \$ g<sup>-1</sup>, which is only affordable for research purpose at this moment. However, with advance in raw materials selection and synthesis technology, lower price even comparable price to synthetic zeolites may be achieved for large scale synthesis of some MOFs in the future.

**Table 3** Cost of the starting materials to produce some MOFs

Adsorbent	Cost <sup>a</sup> /US \$ kg <sup>-1</sup>
CuBTC (HKUST-1)	20.08
CoCo (Co <sub>3</sub> [Co(CN) <sub>6</sub> ] <sub>2</sub> )	35.14
MOF-5 (IRMOF-1)	2.93
Zn/DOBDC (Zn-MOF-74)	1.90
Ni/DOBDC (Ni-MOF-74)	6.48
Co/DOBDC (Co-MOF-74)	13.33
Mg/DOBDC (Mg-MOF-74)	1.19
MIL-100	15.64
MIL-101	4.57
Silica gel	1.00

<sup>a</sup> Costs were estimated from quotes obtained from multiple vendors based on the purchase of one metric ton or greater quantity.

## 5.2 Water stability of MOFs

Another concern for the applications of MOFs in CO<sub>2</sub> capture is their stability toward water vapor. Kusgens *et al.*<sup>130</sup> reported that several MOFs can adsorb a large amount of water and not all of the water molecules can be desorbed because of the chemisorption. They found that both HKUST-1 and DUT-4 are not stable in direct contact with water, whereas the MIL series of MOFs and ZIF-8 do show stability. Low *et al.*<sup>131</sup> used a quantum mechanical method to calculate the activation energies for the reactions between water molecules and metal-oxide bonds. Their results suggest that the strength of the bond between the metal oxide cluster and the bridging linker is important in determining the hydrothermal stability of the MOFs. A steam stability map was also generated for several MOFs and it seems that the stabilities of MOFs increase with the increasing coordination number of the metal atoms from 4 to 6 as shown in Fig. 11.

In addition, HKUST-1 was observed to be stable in O<sub>2</sub> at room temperature, but its crystallinity was reduced in humid environments. The CO<sub>2</sub> adsorption capacity was progressively reduced upon cyclic exposure to water vapor at 30% relative humidity, but leveled out at 75% of its original value after several water adsorption/desorption cycles.<sup>132</sup> Liu *et al.*<sup>36</sup> reported that HKUST-1 and Ni/DOBDC are prone to lose carbon dioxide capacity after repeated H<sub>2</sub>O/CO<sub>2</sub> mixture isotherm measurements. Liang *et al.*<sup>133</sup> reported that Zn<sub>2</sub>(BDC)<sub>2</sub>(Dabco) and Ni<sub>2</sub>(BDC)<sub>2</sub>(Dabco) are stable after O<sub>2</sub> and 30% relative humidity water vapor sorption at 25 °C, but collapsed after 60% relative humidity water vapor sorption at the same

temperature. As a well known MOF which is promising for high pressure CO<sub>2</sub> storage, the framework structure of MOF-177 is not stable upon H<sub>2</sub>O adsorption, which decomposed after exposure to ambient air in 3 days.<sup>134</sup> Recently, Kizzie *et al.*<sup>135</sup> reported that the CO<sub>2</sub> capacity for Mg/DOBDC was drastically diminished after H<sub>2</sub>O breakthrough and subsequent regeneration. In conclusion, water vapor can damage the MOF structures while hindering CO<sub>2</sub> adsorption in MOFs. This is a very important problem that requires urgent solution to advance the applications of MOFs in CO<sub>2</sub> capture.

A straightforward approach to mitigate water effects on stability and CO<sub>2</sub> adsorption is to make MOFs that dislike water, in other words, to create hydrophobic surfaces in MOFs. This can be done through making MOFs with hydrophobic surfaces or modifying hydrophilic MOFs after synthesis. Yang *et al.*<sup>136</sup> synthesized some fluorinated metal-organic frameworks (FMOFs), wherein hydrogen atoms are substituted by fluorine atoms in all ligands. Compared to their non-fluorinated counterparts, FMOFs with fluoro-lined or fluoro-coated channels or cavities have enhanced thermal stability and hydrophobicity. Farha *et al.*<sup>137</sup> synthesized a noncatenated, 3D MOF featuring solvent-capped metal nodes. They replaced the coordinated solvent molecules with various cavity modifiers, including pyridine and its derivatives. The resulting tailored cavities show different adsorption properties and this post-synthetic modification method can be adopted to cover hydrophilic surfaces in some MOFs with hydrophobic molecules, such as pyridine, to reduce H<sub>2</sub>O effects on CO<sub>2</sub> adsorption. Nguyen and Cohen<sup>138</sup> successfully demonstrated that hydrophobic properties can be easily

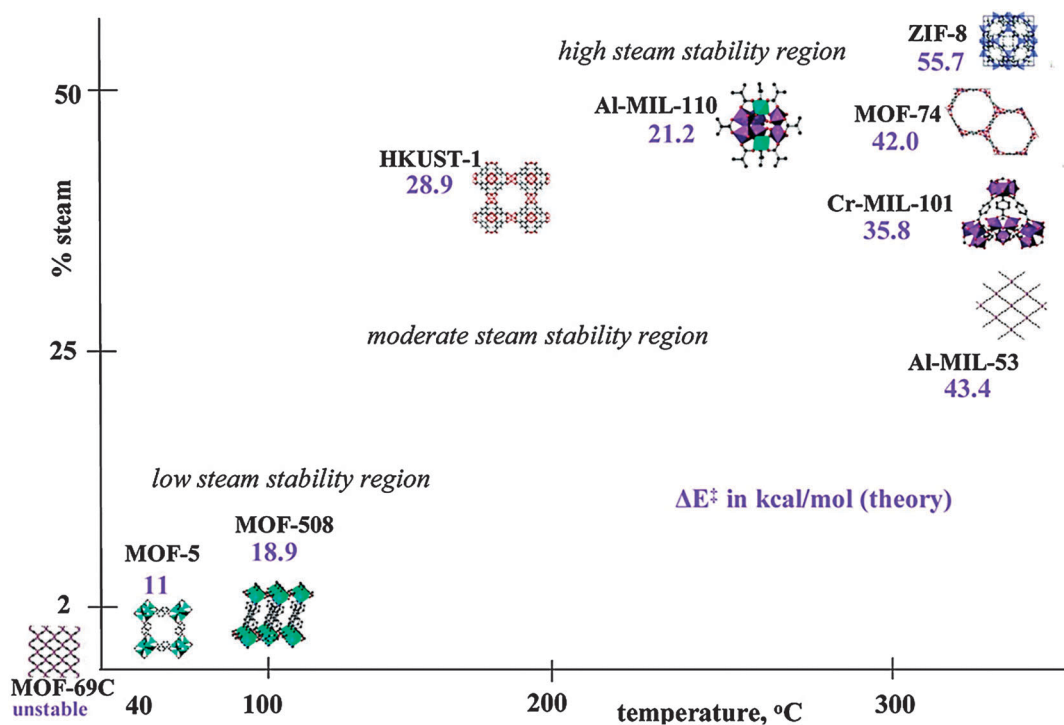


**Fig. 11** Steam stability map for several MOFs. The position of the structure for a given MOF represents its maximum structural stability by XRD measurement. The energy of activation for ligand displacement by a water molecule determined by molecular modeling is in kcal mol<sup>-1</sup>. Reproduced from ref. 131.

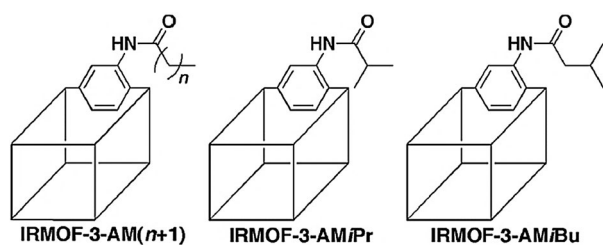


**Fig. 12** Schematic representations of the modified IRMOF-3 after synthesis. One modified organic ligand substituent is shown in each structure. Reproduced from ref. 138.

incorporated within a MOF. They integrated medium to long alkyl groups into IRMOF-3, as shown in Fig. 12, turning the moisture-sensitive MOF into a hydrophobic material which can maintain its structure upon contact with water.

Yang *et al.*<sup>139</sup> synthesized a hydrophobic IRMOF-1 by introducing one or two methyl groups on the BDC moiety and found that the methyl modified IRMOF-1 is significantly less sensitive to water and can maintain its crystal structure compared with the original IRMOF-1.

An engineering solution to relief water effects on the stabilities of MOFs and CO<sub>2</sub> adsorption in them is to install a guard bed loaded with desiccants in front of the main bed loaded with MOFs to remove the majority of water and to take advantage of the MOFs' high CO<sub>2</sub> capacities and selectivities.

Although water can impact CO<sub>2</sub> adsorption in MOFs, many MOFs can retain their structures even after being immersed in water and some organic solvents. For example, HKUST-1 was activated by solvent exchange with dichloromethane after synthesis.<sup>105</sup> The activated HKUST-1 has larger surface area after regeneration than the original sample. This result shows that HKUST-1 is stable toward dichloromethane processing and can retain its structure and porosity. Similarly, Ni/DOBDC can be synthesized in THF/H<sub>2</sub>O and activated with methanol.<sup>123</sup> Another typical MOF, ZIF-8, is stable in diethylformamide and methanol.<sup>140</sup> Moreover, a recently discovered Mn-based MOF can be used as a catalyst for liquid phase chemical reaction without losing its crystal lattice.<sup>141</sup>

In addition to the stability of MOFs toward water vapor and organic solvents, the stability of MOFs toward acid gases, such as SO<sub>x</sub> and NO<sub>x</sub>, the stability of MOFs toward storage, thermal regeneration, and cyclic processing should also be investigated in the future from a practical application point of view.

## 6 Conclusions

MOFs are promising novel adsorbents for CO<sub>2</sub> capture due to their high surface areas, large pore volumes, and easy controllable compositions and pore structures. Progress in adsorption-based CO<sub>2</sub> capture by MOFs has been reviewed and summarized in this paper.

The keys for CO<sub>2</sub> adsorption in MOFs varied with CO<sub>2</sub> pressures. At high pressures, CO<sub>2</sub> capacities depend on surface areas and pore volumes of the MOFs. Therefore, increasing surface areas and pore volumes of MOFs can enhance their CO<sub>2</sub> storage capabilities. At low pressures, CO<sub>2</sub> capacities

depend on the heats of adsorption for CO<sub>2</sub> adsorbed in MOFs.<sup>142</sup> Therefore, increasing the interaction strength between CO<sub>2</sub> molecules and the MOFs, such as introducing unsaturated metal centers, can help increase the CO<sub>2</sub> capacities for MOFs. Besides high CO<sub>2</sub> capacities, many MOFs have high CO<sub>2</sub>/N<sub>2</sub> and CO<sub>2</sub>/CH<sub>4</sub> selectivities which are essential for CO<sub>2</sub> separation from flue gas and natural gas. However, research in further improving CO<sub>2</sub> capacities and/or selectivities, especially under moist conditions, is still necessary for MOFs to clearly stand out from the traditional microporous adsorbents.

One important advantage of MOFs compared to traditional zeolites is their diversities in compositions and crystal structures. Many research studies have shown that either the CO<sub>2</sub> capacities or selectivities or both can be improved or tailored for some MOFs by reducing the pore sizes, such as interpenetration or catenation,<sup>106</sup> modifying the organic linkers, such as amine functionalization,<sup>143</sup> and introducing electrostatic force, such as metal ions exchange.<sup>127</sup> In addition, the post-synthetic method becomes a popular and effective way to endow new properties or change current properties of MOFs to meet specific needs.<sup>138</sup>

Two important issues to be addressed before applying MOFs into practical applications of CO<sub>2</sub> capture are how to synthesize MOFs in bulk with reasonable cost and how to improve the stabilities of MOFs toward water vapor, heat regeneration, and acid gases. The keys to approach addressing the first issue are to scale up the MOF synthesis processes, substitute the synthesized organic linkers with some raw materials in petroleum, and adopt new synthesis and activation procedures to minimize the usage of expensive solvent throughout the processes. Regarding the second issue, new MOFs with hydrophobic surfaces, such as the fluorinated MOFs (FMOFs), may have enhanced hydrothermal stabilities toward their non-fluorinated analogues.<sup>144–146</sup> Changing the surfaces in some MOFs from hydrophilic to hydrophobic is another option to increase their stabilities toward direct contact with water vapor and also may reduce water effects on CO<sub>2</sub> adsorption in the MOFs.<sup>147</sup> More data are needed to better understand and evaluate the stabilities of MOFs toward cyclic processes and acid gases.

Although significant challenges exist in applying MOFs in CO<sub>2</sub> capture, MOFs are still promising novel adsorbents for CO<sub>2</sub> capture.<sup>83,148,149</sup> Because many MOFs have larger CO<sub>2</sub> capacities than benchmark zeolites and water adsorption does not affect CO<sub>2</sub> adsorption in some MOFs as much as in zeolites.<sup>36</sup> Some MOFs have much higher CO<sub>2</sub> selectivities than traditional adsorbents and the CO<sub>2</sub> isotherms for some MOFs are more linear than those of zeolites which indicate larger CO<sub>2</sub> working capacities under the same pressure swing adsorption (PSA) process.<sup>150</sup> Meanwhile, exploring and developing of MOFs is still in its early stage, we can anticipate that new and probably better MOFs for CO<sub>2</sub> capture will be discovered in the near future because of their versatility in chemical compositions and crystal structures. By then, the cost to produce MOFs may gradually approach a level that is affordable to the related industry after adopting some new technology in the synthesis processes. Breakthroughs in developing MOFs with high CO<sub>2</sub> capacities, high selectivities, and high hydrothermal stabilities are still urgently needed.

## Acknowledgements

Jian Liu would like to thank Prof. M. Douglas LeVan at Vanderbilt University for introducing him into gas adsorption in MOFs research. We would like to thank Laboratory Direct Research and U.S. Department of Energy, Office of Fossil Energy for financial support. In addition we would like to thank U.S. Department of Energy, Office of Basic Energy Sciences, Division of Materials Sciences and Engineering under Award KC020105-FWP12152. The Pacific Northwest National Laboratory is operated by Battelle for the U.S. Department of Energy under Contract DE-AC05-76RL01830.

## Notes and references

- H. Q. Yang, Z. H. Xu, M. H. Fan, R. Gupta, R. B. Slimane, A. E. Bland and I. Wright, *J. Environ. Sci.*, 2008, **20**, 14–27.
- R. G. Watts, *Global Warming and the Future of the Earth*, Morgan & Claypool Publishers, Denver, 2007.
- Inventory of U.S. Greenhouse Gas Emissions and Sinks: 1990–2006, Environmental Protection Agency, Washington DC, 2008.
- J. P. Ciferno, T. E. Fout, A. P. Jones and J. T. Murphy, *Chem. Eng. Prog.*, 2009, **105**, 33–41.
- A. Yamasaki, *J. Chem. Eng. Jpn.*, 2003, **36**, 361–375.
- J. T. Yeh, K. P. Resnik, K. Rygle and H. W. Pennline, *Fuel Process. Technol.*, 2005, **86**, 1533–1546.
- X. Xu, C. S. Song, J. M. Andresen, B. G. Miller and A. W. Scaroni, *Energy Fuels*, 2002, **16**, 1463–1469.
- K. T. Chue, J. N. Kim, Y. J. Yoo, S. H. Cho and R. T. Yang, *Ind. Eng. Chem. Res.*, 1995, **34**, 591–598.
- J. L. Soares, H. J. Jos and R. F. P. M. Moreira, *Braz. J. Chem. Eng.*, 2003, **20**, 75–80.
- E. Diaz, E. Munoz, A. Vega and S. Ordonez, *Chemosphere*, 2008, **70**, 1375–1382.
- J. R. Long and O. M. Yaghi, *Chem. Soc. Rev.*, 2009, **38**, 1213–1214.
- M. Eddaoudi, D. B. Moler and H. Li, *Acc. Chem. Res.*, 2001, **34**, 319–330.
- D. J. Tranchemontagne, J. L. Mendoza-Cortes, M. O’Keeffe and O. M. Yaghi, *Chem. Soc. Rev.*, 2009, **38**, 1257–1283.
- H. L. Li, M. Eddaoudi, M. O’Keeffe and O. M. Yaghi, *Nature*, 1999, **402**, 276–279.
- J. L. C. Rowsell, E. C. Spencer, J. Eckert, J. A. K. Howard and O. M. Yaghi, *Science*, 2005, **309**, 1350–1354.
- M. Eddaoudi, J. Kim, N. L. Rosi, D. T. Vodak, J. Wachter, M. O’Keeffe and O. M. Yaghi, *Science*, 2002, **295**, 469–472.
- N. L. Rosi, J. Eckert, M. Eddaoudi, D. T. Vodak, J. Kim, M. O’Keeffe and O. M. Yaghi, *Science*, 2003, **300**, 1127–1129.
- U. Mueller, M. Schubert, F. Teich, H. Puetter, K. Schierle-Arndt and J. Pastre, *J. Mater. Chem.*, 2006, **16**, 626–636.
- R. Babarao and J. W. Jiang, *Langmuir*, 2008, **24**, 6270–6278.
- H. L. Li, C. E. Davis, T. L. Groy, D. G. Kelley and O. M. Yaghi, *J. Am. Chem. Soc.*, 1998, **120**, 2186–2187.
- D. Britt, H. Furukawa, B. Wang, T. G. Glover and O. M. Yaghi, *Proc. Natl. Acad. Sci. U. S. A.*, 2009, **106**, 20637–20640.
- T. G. Glover, G. W. Peterson, B. J. Schindler, D. Britt and O. M. Yaghi, *Chem. Eng. Sci.*, 2011, **66**, 163–170.
- P. D. C. Dietzel, Y. Morita, R. Blom and H. Fjellvag, *Angew. Chem., Int. Ed.*, 2005, **44**, 6354–6358.
- D. J. Collins and H. C. Zhou, *J. Mater. Chem.*, 2007, **17**, 3154–3160.
- M. Eddaoudi, J. Kim and N. Rosi, *et al.*, *Science*, 2002, **295**, 469–472.
- O. M. Yaghi, M. O’Keeffe and N. W. Ockwig, *et al.*, *Nature*, 2003, **423**, 705–714.
- M. O’Keeffe, *Chem. Soc. Rev.*, 2009, **38**, 1215–1217.
- S. Kitagawa and R. Matsuda, *Coord. Chem. Rev.*, 2007, **251**, 2490–2509.
- G. Ferey, *Chem. Soc. Rev.*, 2008, **37**, 191–214.
- M. P. Suh, Y. E. Cheon and E. Y. Lee, *Coord. Chem. Rev.*, 2008, **252**, 1007–1026.
- Z. Wang and S. M. Cohen, *Chem. Soc. Rev.*, 2009, **38**, 1315–1329.
- R. Babarao and J. W. Jiang, *Langmuir*, 2008, **24**, 5474–5484.
- Q. Y. Yang, C. L. Zhong and J. F. Chen, *J. Phys. Chem. C*, 2008, **112**, 1562–1569.
- Z. X. Zhao, Z. Li and Y. S. Lin, *Ind. Eng. Chem. Res.*, 2009, **48**, 10015–10020.
- F. Salles, H. Jobic, G. Maurin, M. M. Koza, P. L. Llewellyn, T. Devic, C. Serre and G. Ferey, *Phys. Rev. Lett.*, 2008, **100**, 245901.
- J. Liu, Y. Wang, A. I. Benin, P. Jakubczak, R. R. Willis and M. D. LeVan, *Langmuir*, 2010, **26**, 14301–14307.
- O. M. Yaghi and Q. Li, *MRS Bull.*, 2009, **34**, 682–690.
- L. J. Murray, M. Dinc and J. R. Long, *Chem. Soc. Rev.*, 2009, **38**, 1294–1314.
- J. R. Li, R. J. Kuppler and H. C. Zhou, *Chem. Soc. Rev.*, 2009, **38**, 1477–1504.
- J. Y. Lee, O. K. Farha, J. Roberts, K. A. Scheidt, S. T. Nguyen and J. T. Hupp, *Chem. Soc. Rev.*, 2009, **38**, 1450–1459.
- Y. Q. Zou, A. I. Abdel-Fattah, H. W. Xu, Y. S. Zhao and D. D. Hickmott, *CrystEngComm*, 2010, **12**, 1337–1353.
- G. Ferey, C. Serre, T. Devic, G. Maurin, H. Jobic, P. L. Llewellyn, G. De Weireld, A. Vimont, M. Daturif and J. S. Chang, *Chem. Soc. Rev.*, 2011, **40**, 550–562.
- S. Keskin, T. M. Van Heest and D. S. Sholl, *ChemSusChem*, 2010, **3**, 879–891.
- L. M. Robeson, *J. Membr. Sci.*, 1991, **62**, 165–185.
- C. M. Zimmerman, A. Singh and W. J. Koros, *J. Membr. Sci.*, 1997, **137**, 145–154.
- R. V. Siriwardane, M. S. Shen, E. P. Fisher and J. A. Poston, *Energy Fuels*, 2001, **15**, 279–284.
- D. Aaron and C. Tsouris, *Sep. Sci. Technol.*, 2005, **40**, 321–348.
- J. D. Figueroa, T. Fout, S. Plasynski, H. Mellvried, R. D. Srivastava and D. Rameshwar, *Int. J. Greenhouse Gas Control*, 2008, **2**, 9–20.
- A. R. Millward and O. M. Yaghi, *J. Am. Chem. Soc.*, 2005, **127**, 17998–17999.
- T. Loiseau, C. Serre, C. Huguenard, G. Fink, F. Taulelle, M. Henry, T. Bataille and G. Ferey, *Chem.–Eur. J.*, 2004, **10**, 1373–1382.
- S. Bourrelly, P. L. Llewellyn, C. Serre, F. Millange, T. Loiseau and G. Ferey, *J. Am. Chem. Soc.*, 2005, **127**, 13519–13521.
- P. K. Thallapally, J. Tian, M. R. Kishan, C. A. Fernandez, S. J. Dalgarno, P. B. McGrail, J. E. Warren and J. L. Atwood, *J. Am. Chem. Soc.*, 2008, **130**, 16842–16843.
- P. L. Llewellyn, S. Bourrelly, C. Serre, A. Vimont, M. Daturi and L. Hamon, *et al.*, *Langmuir*, 2008, **24**, 7245–7250.
- K. Koh, A. G. Wong-Foy and A. J. Matzger, *Angew. Chem., Int. Ed.*, 2008, **47**, 677–680.
- B. Mu, P. M. Schoencker and K. S. Walton, *J. Phys. Chem. C*, 2010, **114**, 6464–6471.
- O. K. Farha, A. O. Yazaydn, I. Eryazici, C. D. Malliakas, B. G. Hauser, M. G. Kanatzidis, S. T. Nguyen, R. Q. Snurr and J. T. Hupp, *Nat. Chem.*, 2010, **2**, 944–948.
- H. Furukawa, N. Ko, Y. B. Go, N. Aratani, S. B. Choi, E. Choi, A. O. Yazaydin, R. Q. Snurr, M. O’Keeffe, J. Kim and O. M. Yaghi, *Science*, 2010, **329**, 424–428.
- J. Moellmer, A. Moeller, F. Dreisbach, R. Glaeser and R. Staudt, *Microporous Mesoporous Mater.*, 2011, **138**, 140–148.
- D. Saha, Z. B. Bao, F. Jia and S. G. Deng, *Environ. Sci. Technol.*, 2009, **44**, 1820–1826.
- B. Arstad, H. Fjellvag, K. O. Kongshaug, O. Swang and R. Blom, *Adsorption*, 2008, **14**, 755–762.
- S. Surble, F. Millange, C. Serre, T. Duren, M. Latroche, S. Bourrelly, P. L. Llewellyn and G. Ferey, *J. Am. Chem. Soc.*, 2006, **128**, 14889–14896.
- M. Xue, Y. Liu, R. M. Schaffino, S. C. Xiang, X. J. Zhao, G. S. Zhu, S. L. Qiu and B. L. Chen, *Inorg. Chem.*, 2009, **48**, 4649–4651.
- M. Park, D. Moon, J. W. Yoon, J. S. Chang and M. S. Lah, *Chem. Commun.*, 2009, 2026–2028.
- A. P. Nelson, O. K. Farha, K. L. Mulfort and J. T. Hupp, *J. Am. Chem. Soc.*, 2009, **131**, 458–460.
- A. O. Yazaydn, R. Q. Snurr, T. H. Park, K. Koh, J. Liu, M. D. LeVan, A. I. Benin, P. Jakubczak, M. Lanuza,

- D. B. Galloway, J. J. Low and R. R. Willis, *J. Am. Chem. Soc.*, 2009, **131**, 18198–18199.
- 66 P. Aprea, D. Caputo, N. Gargiulo, F. Iucolano and F. Pepe, *J. Chem. Eng. Data*, 2010, **55**, 3655–3661.
- 67 S. R. Caskey, A. G. Wong-Foy and A. J. Matzger, *J. Am. Chem. Soc.*, 2008, **130**, 10870–10871.
- 68 J. R. Li, Y. Tao, Q. Yu, X. H. Bu, H. Sakamoto and S. Kitagawa, *Chem.–Eur. J.*, 2008, **14**, 2771–2776.
- 69 B. Liu and B. Smit, *Langmuir*, 2009, **25**, 5918–5926.
- 70 D. Wu, Q. Xu, D. H. Liu and C. L. Zhong, *J. Phys. Chem. C*, 2010, **114**, 16611–16617.
- 71 Q. Y. Yang, L. L. Ma, C. L. Zhong, X. H. An and D. H. Liu, *J. Phys. Chem. C*, 2011, **115**, 2790–2797.
- 72 V. Finsy, L. Ma, L. Alaerts, D. E. De Vos, G. V. Baron and J. F. M. Denayer, *Microporous Mesoporous Mater.*, 2009, **120**, 221–227.
- 73 S. Couck, J. F. M. Denayer, G. V. Baron, T. Remy, J. Gascon and F. Kapteijn, *J. Am. Chem. Soc.*, 2009, **131**, 6326–6327.
- 74 Q. Y. Yang and C. L. Zhong, *ChemPhysChem*, 2006, **7**, 1417–1421.
- 75 A. Martin-Calvo, E. Garcia-Perez, J. M. Castillo and S. Calero, *Phys. Chem. Chem. Phys.*, 2008, **10**, 7085–7091.
- 76 L. Hamon, E. Jolimaitre and G. D. Pirngruber, *Ind. Eng. Chem. Res.*, 2010, **49**, 7497–7503.
- 77 S. Keskin and D. S. Sholl, *J. Phys. Chem. C*, 2007, **111**, 14055–14059.
- 78 E. V. Perez, K. J. Balkus, J. P. Ferraris and I. H. Musselman, *J. Membr. Sci.*, 2009, **328**, 165–173.
- 79 Q. Xu, D. H. Liu, Q. Y. Yang, C. L. Zhong and J. G. Mi, *J. Mater. Chem.*, 2010, **20**, 706–714.
- 80 Y. S. Bae, B. G. Hauser, O. K. Farha, J. T. Hupp and R. Q. Snurr, *Microporous Mesoporous Mater.*, 2011, **141**, 231–235.
- 81 Z. B. Bao, L. A. Yu, Q. L. Ren, X. Y. Lu and S. G. Deng, *J. Colloid Interface Sci.*, 2011, **353**, 549–556.
- 82 Y. F. Chen and J. W. Jiang, *ChemSusChem*, 2010, **3**, 982–988.
- 83 Z. X. Chen, S. C. Xiang, H. D. Arman, P. Li, S. Tidrow, D. Y. Zhao and B. L. Chen, *Eur. J. Inorg. Chem.*, 2010, 3745–3749.
- 84 J. R. Li, Y. G. Ma, M. C. McCarthy, J. Sculley, J. M. Yu, H. K. Jeong, P. B. Balbuena and H. C. Zhou, *Coord. Chem. Rev.*, 2011, **255**, 1791–1823.
- 85 S. Cavenati, C. A. Grande and A. E. Rodrigues, *Ind. Eng. Chem. Res.*, 2008, **47**, 6333–6335.
- 86 Q. Y. Yang, C. Y. Xue, C. L. Zhong and J. F. Chen, *AIChE J.*, 2007, **53**, 2832–2840.
- 87 R. Babarao and J. W. Jiang, *Ind. Eng. Chem. Res.*, 2011, **50**, 62–68.
- 88 L. Bastin, P. S. Barcia, E. J. Hurtado, J. A. C. Silva, A. E. Rodrigues and B. Chen, *J. Phys. Chem. C*, 2007, **112**, 1575–1581.
- 89 R. Babarao and J. W. Jiang, *J. Am. Chem. Soc.*, 2009, **131**, 11417–11425.
- 90 A. Phan, C. J. Doonan, F. J. Uribe-Romo, C. B. Knobler, M. O’Keeffe and O. M. Yaghi, *Acc. Chem. Res.*, 2010, **43**, 58–67.
- 91 Y. F. Chen, J. Y. Lee, R. Babarao, J. Li and J. W. Jiang, *J. Phys. Chem. C*, 2010, **114**, 6602–6609.
- 92 H. H. Wu, R. S. Reali, D. A. Smith, M. C. Trachtenberg and J. Li, *Chem.–Eur. J.*, 2010, **16**, 13951–13954.
- 93 Y. S. Bae, K. L. Mulfort, H. Frost, P. Ryan, S. Punnathanam, L. J. Broadbelt, J. T. Hupp and R. Q. Snurr, *Langmuir*, 2008, **24**, 8592–8598.
- 94 M. Xue, Z. J. Zhang, S. C. Xiang, Z. Jin, C. D. Liang, G. S. Zhu, S. L. Qiu and B. L. Chen, *J. Mater. Chem.*, 2010, **20**, 3984–3988.
- 95 A. O. Yazaydin, A. I. Benin, S. A. Faheem, P. Jakubczak, J. J. Low, R. R. Willis and R. Q. Snurr, *Chem. Mater.*, 2009, **21**, 1425–1430.
- 96 Y. F. Chen, R. Babarao, S. I. Sandler and J. W. Jiang, *Langmuir*, 2010, **26**, 8743–8750.
- 97 J. Liu, A. I. Benin, A. M. B. Furtado, P. Jakubczak, R. R. Willis and M. D. LeVan, *Langmuir*, 2011, **27**, 11451–11456.
- 98 A. C. Kizzie, A. G. Wong-Foy and A. J. Matzger, *Langmuir*, 2011, **27**, 6368–6373.
- 99 R. T. Yang, *Adsorbents: Fundamentals and Applications*, John Wiley & Sons, Inc, New Jersey, 2003.
- 100 B. J. Schindler and M. D. LeVan, *Carbon*, 2008, **46**, 644–648.
- 101 J. Liu and M. D. LeVan, *Carbon*, 2009, **47**, 3415–3423.
- 102 J. Liu and M. D. LeVan, *Carbon*, 2010, **48**, 3454–3462.
- 103 H. Frost, T. Duren and R. Q. Snurr, *J. Phys. Chem. B*, 2006, **110**, 9565–9570.
- 104 B. Chen, M. Eddaoudi, S. T. Hyde, M. O’Keeffe and O. M. Yaghi, *Science*, 2001, **291**, 1021–1023.
- 105 J. L. C. Rowsell and O. M. Yaghi, *J. Am. Chem. Soc.*, 2006, **128**, 1304–1315.
- 106 B. Liu, Q. Yang, C. Xue, C. Zhong, B. Chen and B. Smit, *J. Phys. Chem. C*, 2008, **112**, 9854–9860.
- 107 S. Keskin and D. S. Sholl, *Langmuir*, 2009, **25**, 11786–11795.
- 108 Y. E. Cheon, J. Park and M. P. Suh, *Chem. Commun.*, 2009, 5436–5438.
- 109 J. Kim, S. T. Yang, S. B. Choi, J. Sim and W. S. Ahn, *J. Mater. Chem.*, 2011, **21**, 3070–3076.
- 110 J. J. Zhang, L. Wojtas, R. W. Larsen, M. Eddaoudi and M. J. Zaworotko, *J. Am. Chem. Soc.*, 2009, **131**, 17040–17041.
- 111 N. A. Ramsahye, G. Maurin, S. Bourrelly, P. L. Llewellyn, T. Devic, C. Serre, T. Loiseau and G. Ferey, *Adsorption*, 2007, **13**, 461–467.
- 112 N. A. Ramsahye, G. Maurin, S. Bourrelly, P. L. Llewellyn, C. Serre, T. Loiseau, T. Devic and G. Ferey, *J. Phys. Chem. C*, 2008, **112**, 514–520.
- 113 C. Serre, S. Bourrelly, A. Vimont, N. A. Ramsahye, G. Maurin, P. L. Llewellyn, M. Daturi, Y. Filinchuk, O. Leynaud, P. Barnes and G. Ferey, *Adv. Mater.*, 2007, **19**, 2246–2251.
- 114 A. Vimont, A. Travert, P. Bazin, J. C. Lavalley, M. Daturi, C. Serre, G. Ferey, S. Bourrelly and P. L. Llewellyn, *Chem. Commun.*, 2007, 3291–3293.
- 115 W. Mu, D. H. Liu, Q. Y. Yang and C. L. Zhong, *Microporous Mesoporous Mater.*, 2010, **130**, 76–82.
- 116 R. Vaidhyanathan, S. S. Iremonger, K. W. Dawson and G. K. H. Shimizu, *Chem. Commun.*, 2009, 5230–5232.
- 117 A. Demessence, D. M. D’Alessandro, M. L. Foo and J. R. Long, *J. Am. Chem. Soc.*, 2009, **131**, 8784–8786.
- 118 B. S. Zheng, J. F. Bai, J. G. Duan, L. Wojtas and M. J. Zaworotko, *J. Am. Chem. Soc.*, 2011, **133**, 748–751.
- 119 Z. Q. Wang and S. M. Cohen, *J. Am. Chem. Soc.*, 2009, **131**, 16675–16677.
- 120 J. An, S. J. Geib and N. L. Rosi, *J. Am. Chem. Soc.*, 2010, **132**, 38–39.
- 121 J. An and N. L. Rosi, *J. Am. Chem. Soc.*, 2010, **132**, 5578–5579.
- 122 Y. S. Bae, O. K. Farha, A. M. Spokoyny, C. A. Mirkin, J. T. Hupp and R. Q. Snurr, *Chem. Commun.*, 2008, 4135–4137.
- 123 P. D. C. Dietzel, V. Besikiotis and R. Blom, *J. Mater. Chem.*, 2009, **19**, 7362–7370.
- 124 K. Sumida, S. Horike, S. S. Kaye, Z. R. Herm, W. L. Queen, C. M. Brown, F. Grand-jean, G. J. Long, A. Dailly and J. R. Long, *Chem. Sci.*, 2010, **1**, 184–191.
- 125 J. B. Lin, J. P. Zhang and X. M. Chen, *J. Am. Chem. Soc.*, 2010, **132**, 6654–6656.
- 126 R. Babarao, J. W. Jiang and S. I. Sandler, *Langmuir*, 2009, **25**, 5239–5247.
- 127 J. A. Botas, G. Calleja, M. Sanchez-Sanchez and M. G. Orcajo, *Langmuir*, 2010, **26**, 5300–5303.
- 128 Z. H. Xiang, Z. Hu, D. P. Cao, W. T. Yang, J. M. Lu, B. Y. Han and W. C. Wang, *Angew. Chem., Int. Ed.*, 2011, **50**, 491–494.
- 129 Y. S. Bae, O. K. Farha, J. T. Hupp and R. Q. Snurr, *J. Mater. Chem.*, 2009, **19**, 2131–2134.
- 130 P. Kusgens, M. Rose, I. Senkovska, H. Frode, A. Henschel, S. Siegle and S. Kaskel, *Microporous Mesoporous Mater.*, 2009, **120**, 325–330.
- 131 J. J. Low, A. I. Benin, P. Jakubczak, J. F. Abrahamian, S. A. Faheem and R. R. Willis, *J. Am. Chem. Soc.*, 2009, **131**, 15834–15842.
- 132 Z. J. Liang, M. Marshall and A. L. Chaffee, *Energy Fuels*, 2009, **23**, 2785–2789.
- 133 Z. J. Liang, M. Marshall and A. L. Chaffee, *Microporous Mesoporous Mater.*, 2010, **132**, 305–310.
- 134 Y. Li and R. T. Yang, *Langmuir*, 2007, **23**, 12937–12944.
- 135 A. C. Kizzie, A. G. Wong-Foy and A. J. Matzger, *Langmuir*, 2011, **27**, 6368–6373.
- 136 C. Yang, X. P. Wang and M. A. Omary, *J. Am. Chem. Soc.*, 2007, **129**, 15454–15455.
- 137 O. K. Farha, K. L. Mulfort and J. T. Hupp, *Inorg. Chem.*, 2008, **47**, 10223–10225.
- 138 J. G. Nguyen and S. M. Cohen, *J. Am. Chem. Soc.*, 2010, **132**, 4560–4561.
- 139 J. Yang, A. Grzech, F. M. Mulder and T. J. Dingemans, *Chem. Commun.*, 2011, **47**, 5244–5246.

- 140 K. S. Park, Z. Ni, A. P. Cote, J. Y. Choi, R. Huang, F. J. Uribe-Romo, H. K. Chae, M. O'Keeffe and O. M. Yaghi, *Proc. Natl. Acad. Sci. U. S. A.*, 2006, **103**, 10186–10191.
- 141 S. Horike, M. Dinca, K. Tamaki and J. R. Long, *J. Am. Chem. Soc.*, 2008, **130**, 5854–5855.
- 142 H. Frost and R. Q. Snurr, *J. Phys. Chem. C*, 2007, **111**, 18794–18803.
- 143 R. Vaidhyanathan, S. S. Iremonger, G. K. H. Shimizu, P. G. Boyd, S. Alavi and T. K. Woo, *Science*, 2010, **330**, 650–653.
- 144 C. Yang, X. P. Wang and M. A. Omary, *J. Am. Chem. Soc.*, 2007, **129**, 15454–15455.
- 145 C. Yang, X. P. Wang and M. A. Omary, *Angew. Chem., Int. Ed.*, 2009, **48**, 2500–2505.
- 146 C. Yang, U. Kaipa, Q. Z. Mather, X. Wang, V. Nesterov, A. F. Venero and M. A. Omary, *J. Am. Chem. Soc.*, 2011, **133**, 18094–18097.
- 147 J. Yang, A. Grzech, F. M. Mulder and T. J. Dingemans, *Chem. Commun.*, 2011, **47**, 5244–5246.
- 148 J. R. Li, J. Sculley and H. C. Zhou, *Chem. Rev.*, 2011, DOI: 10.1021/cr200190s.
- 149 Y. S. Bae and R. Q. Snurr, *Angew. Chem., Int. Ed.*, 2011, **50**, 2–13.
- 150 J. A. Mason, K. Sumida, Z. R. Herm, R. Krishna and J. R. Long, *Energy Environ. Sci.*, 2011, **4**, 3030–3040.